Journal of Colloid and Interface Science 497 (2017) 165–171

Contents lists available at ScienceDirect

Journal of Colloid and Interface Science

journal homepage: www.elsevier.com/locate/jcis

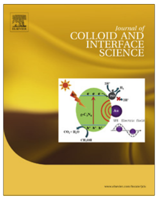

Regular Article

Preparation and application of carbon-nanodot@NaCl composite phosphors with strong green emission

Yuechen Zhai [a], Ding Zhou [a,*], Pengtao Jing [a], Di Li [a], Haibo Zeng [b], Songnan Qu [a,*]

[a] *State Key Laboratory of Luminescence and Applications, Changchun Institute of Optics, Fine Mechanics and Physics, Chinese Academy of Sciences, Changchun 130033, China*
[b] *Institute of Optoelectronics & Nanomaterials, College of Material Science and Engineering, Nanjing University of Science and Technology, Nanjing 210094, China*

GRAPHICAL ABSTRACT

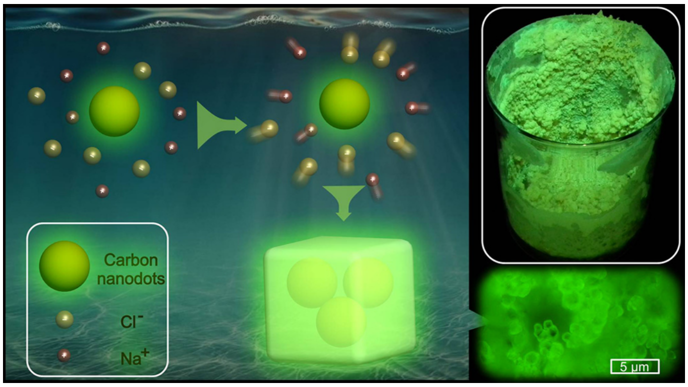

ARTICLE INFO

Article history:
Received 27 December 2016
Revised 18 February 2017
Accepted 1 March 2017
Available online 2 March 2017

Keywords:
Carbon dots
NaCl
Composite phosphors
High photostability
White light-emitting diodes

ABSTRACT

Luminescent carbon nanodots (CDots) have attracted much attention, but their luminescence is usually quenched in solid state. Efficient green or yellow emissive CDot-based phosphors are scarce. In this work, green emissive CDot@NaCl composite phosphors were fabricated through a convenient, low cost and eco-friendly way by embedding green emissive CDots (g-CDot) in NaCl crystals. With the protection of NaCl host, the g-CDot@NaCl composite phosphors exhibit good photostability, significant resistance to organic solvents, and improved photoluminescence quantum yields up to 25%. White light-emitting diodes with tunable color temperatures (3944–5478 K) and CIE coordinates have been realized based on the g-CDot@NaCl composite phosphors.

1. Introduction

White light-emitting diodes (WLEDs) as emerging lighting sources possess many competitive advantages, such as energy-saving, long working life time, low power consumption, fast response time, compact size and so forth [1–3]. Commercial WLEDs are usually based on blue-emitting chips and luminescent phosphors [1,4]. The performances of WLEDs are greatly dependent on phosphors. Efficient green or yellow light-emitting phosphors are strongly needed. Traditional phosphors are based on the non-renewable rare earth materials [5]. However, the fabrication of the traditional phosphors is highly energy consuming, and exploitation of rare earth is potentially harmful for environment.

---

* Corresponding authors.
E-mail addresses: qusn@ciomp.ac.cn (S. Qu), zhouding@ciomp.ac.cn (D. Zhou).

http://dx.doi.org/10.1016/j.jcis.2017.03.007
0021-9797/

Semiconductor quantum dots (QDs), as a new type of phosphors, have been used in WLEDs in recent years [6]. However, the QDs usually contain heavy metal elements, leading to toxicity concerns [7]. Thus, it is of great scientific interest to exploit new phosphors which are low-toxic, low-cost and eco-friendly, as alternative phosphors for WLEDs.

Carbon nanodots (CDots), as emerging luminescent nanomaterials, have attracted more and more attention in many fields, such as biosensors, bioimaging, optoelectronic devices, drug delivery and light-emitting devices [8–20]. CDots possess several remarkable advantages, such as biocompatibility, low toxicity, chemical stability, photostability, and multicolor emission [21–43]. Currently, CDots have shown potential to be as a color conversion layer for WLEDs [44]. Nevertheless, owing to self-quenching in the aggregated state [45], suitable matrices are utilized to disperse CDots uniformly in solid state [26]. Rogach et al. embedded blue emissive CDots in polyhedral oligomeric silsesquioxane matrices to fabricate deep blue-emitting solid-state phosphors and combined this phosphors with green- and red-emitting CdTe@NaCl powders to realize WLEDs [46]. Rhee et al. used CDots to fabricate freestanding films based on poly (methylmethacrylate) matrices, and combine the films with an InGaN blue emissive chip to achieve WLEDs [31]. In our previous work, we used green emissive CDots (g-CDots) and starch to synthesize eco-friendly green emissive phosphors [47]. However, organic matrices usually have poor thermal instability. Green or yellow emissive phosphors only based on CDots and inorganic matrices are scarce. Thus, it is important to develop efficient green or yellow emissive CDot-based composite phosphors.

In this work, a simple and convenient synthetic method could put forward to synthesize green emissive g-CDot@NaCl composite phosphors with photoluminescence quantum yields (PLQYs) up to 25%. By virtue of inorganic matrices, the composite phosphors possess excellent photostability, resistance to organic solvents, and structural stability. Therefore, WLEDs with tunable color temperatures and Commission Internationale de L'Eclairage (CIE) coordinates could be realized based on the g-CDot@NaCl composite phosphors.

2. Results and discussion

The g-CDots are synthesized from citric acid and urea by microwave-assisted method [48]. As seen from Fig. S1a, the UV–vis absorption peak of g-CDots solution locates at 410 nm. Under sunlight, its diluted solution presents clearly faint yellow color. When irradiated by UV light, the solution emits strong green luminescence. Fig. S1b shows the excitation-emission matrix of g-CDots dilute aqueous solution, it can be seen that the maximum emission of g-CDots aqueous solution locates at 522 nm with the PLQY of 14% under the 405 nm light.

In order to maintain stable and strong luminescence of g-CDots in solid state, the g-CDots are embedded in NaCl crystals for preventing the aggregation of g-CDots. As described in experimental section, the method of preparing g-CDot@NaCl composite phosphors is very simple. Upon slowly evaporating the as-prepared g-CDots and NaCl saturated aqueous solution, lots of yellow microcrystals with strong green luminescence from the embedded g-CDots gradually grow along the wall of beaker (Fig. 1a and b). For removing the absorbed g-CDots on the surface, the as-prepared microcrystals are washed by ethanol, where g-CDots could be dissolved into ethanol. As seen from the Fig. 1c, the diffuse reflection absorption peak and the emission peak of g-CDot@NaCl composite phosphors locate at 410 and 510 nm, respectively, consisting with the optical properties of initial g-CDots. It is worth mentioning that pure NaCl has no PL emission (Fig. S2), indicating the successful incorporation of g-CDot into the composite phosphors. More meaningfully, under 405 nm excitation, PLQYs of the g-CDot@NaCl composite phosphors could reach 25%. The increased PLQYs is mainly because of less energy loss compared with g-CDots aqueous solution. Water, as a protic solvent, could deteriorate the fluorescence of g-CDot by proton transfer dynamics, whereas there is no proton transfer process in the solid-state composite phosphors, resulting in higher PLQYs [49,50]. This conclusion can be further proved by investigating their PL decay curves (Fig. 2a) [47]. The results in Fig. 2b indicate the luminescence lifetime of the composite phosphors is longer than that of g-CND aqueous solution. Therefore, the g-CDots should be well separately embedded in NaCl matrix with effectively avoiding energy loss induced by water molecules, resulting in enhanced PLQYs. In addition, the excitation-dependent PL emission behavior of g-CDots is also preserved in the g-CDot@NaCl composite phosphors. As shown in Fig. 3, the composite phosphors exhibit turquoise, green, and red, when being excited by UV, blue, and green light.

To further characterize the morphorlogy and structure of the g-CDot@NaCl composite phosphors, scanning electron microscopy (SEM), X-ray powder diffraction (XRD) and energy dispersive spectra (EDS) investigations are carried out. By analyzing the images of SEM images (Fig. 4a and b), the morphology of composite

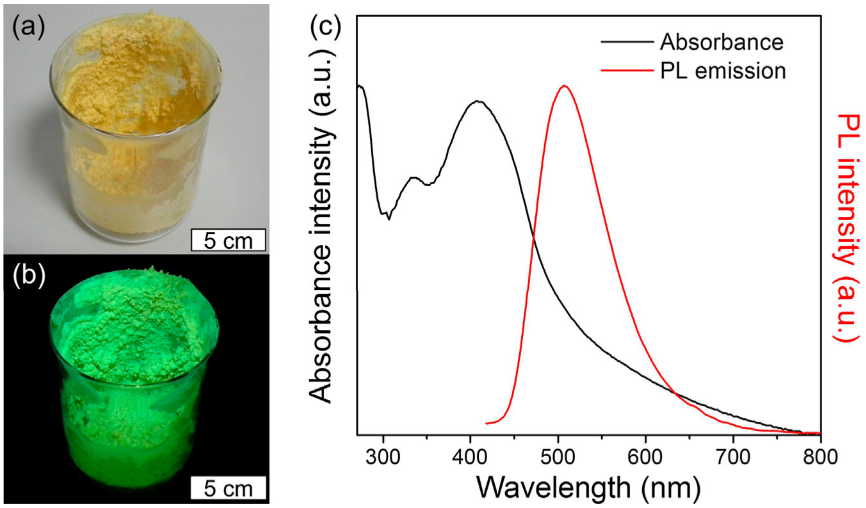

Fig. 1. (a) Optical and (b) fluorescent images of resulting g-CDot@NaCl composite phosphors. (c) Diffuse reflection absorption spectra and PL emission spectra of g-CDot@NaCl composite phosphors.

phosphors is a cubic structure, consisting with the classical structure of NaCl. And, their size are about 2–5 μm, therewith g-CDots are hardly observed owing to the nanosize of g-CDots (2–5 nm) [48]. Furthermore, as seen from Fig. 4c, XRD patterns indicated that the lattice parameters of the g-CDot@NaCl composite phosphors fitted well to the cubic structure of bulk NaCl crystal. There are no characteristic diffraction peaks of g-CDots in the XRD pattern, as they are rather weak and overlap with those of crystalline NaCl crystal. On the other hand, EDS pattern demonstrates the existence of C, N and O elements in the phosphors (Fig. 4d). Since the composite phosphors are deposited on a pure silicon slice, these elements should be originating from g-CND. Based on the above observation, it would be safely concluded that the composite phosphors are comprised of NaCl and g-CDots, where NaCl serves as matrix. Moreover, according to the EDS pattern, the ratio of g-CDots in the phosphors is about 13.5 wt%.

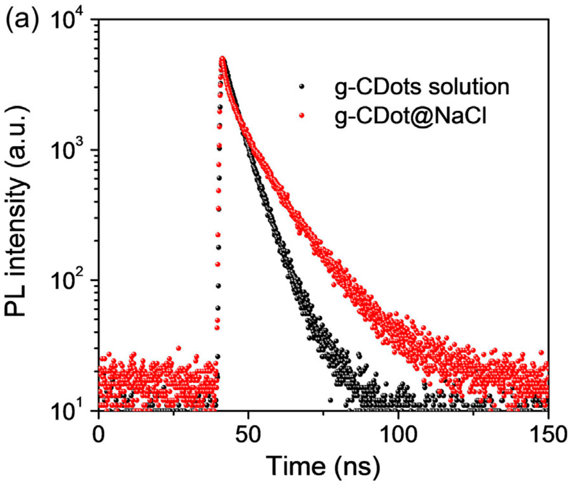

(b)

	τ_1 (ns)	A_1 (%)	τ_2 (ns)	A_2 (%)	τ_{ave} (ns)	χ^2
g-CDots solution	4.91	76.8	9.82	23.2	6.05	1.1
g-CDot@NaCl	1.86	20.1	11.84	79.9	9.84	1.2

Fig. 2. Time-resolved luminescence decay curves collected at 520 nm for g-CDots aqueous solution (black sphere) and g-CDots@NaCl composite phosphors (red sphere) under 405 nm excitation. The average lifetimes were calculated using the equation $\tau_{ave} = \sum_{i=1}^{n} a_i \tau_i$.

As g-CDots itself have been demonstrated to be well resistant against UV light irradiation, the PL emission of g-CDot@NaCl composite phosphors are expected to possess good photostability against UV light irradiation [47]. To prove this issue, the photostability of the g-CDot@NaCl composite phosphors is evaluated using a UV light (1.6 W/cm^2), where fluorescein sodium, a well-known commercial fluorescent dye, is chosen as a control. As seen from Fig. S3, the UV light used in the test is harmful to all samples. At first 5 min, the PL intensity of fluorescein sodium falls to 80% quickly, and its PL intensity losses more than half after 20 min. After 65 min, the PL intensity of fluorescein sodium is almost quenched. On the contrary, the PL intensity of g-CDot@NaCl composite phosphors reduces less than 10% at first 5 min. Then, the decay rate of its PL intensity slows down. As a consequence of this, the PL intensity of phosphors could be retained more than 80% after 65 min. Therefore, g-CDot@NaCl composite phosphors have good ability of resisting against UV light, which is a key issue in fabricating LEDs with long-term lifetime. Moreover, the thermal stability of the composite phosphors is also tested by measuring *in situ* the PL emission spectra (Fig. S4). After heating to 100 °C for 30 min and cooling down to room temperature, the PL emission spectra are nearly unchanged, indicating the good thermal stability of the composite phosphors (Figure S4b).

Besides the good photostability and thermal stability, the composite phosphors also possess resistance toward the organic solvents under the protection of NaCl matrix. As we can see from Fig. 5a1, the g-CDot@NaCl composite phosphors cannot be decomposed in the chloroform, and their PL properties could be preserved very well (Fig. 5a2). The supernatant solution possesses no PL emissions, indicating insolubility of the hybrid phosphors in these solvents (Fig. 5a). This excellent solvent resistance of the composite phosphors allows us to mix theses with various packaging materials when processed toward LEDs without PL emission change. In order to confirm this proposal, the g-CDot@NaCl composite phosphors are mixed with polydimethylsiloxane (PDMS) to form a bulk material (Fig. 5). It is found that the bulk material preserve strong PL emission of the composite phosphors under UV light. Meanwhile, due to the protection of PDMS, the as-prepared bulk material posse excellent stability in the humid conditions, even being immersed in water (Fig. S5). Furthermore, even if the bulk material is stretched strongly by external mechanical force, PL property has no variation, indicating a good structural stability (Fig. 5b). In all, the excellent solvent, structure, and photostability of current composite phosphors allow the further application in photoelectric devices.

Based on the above advantages, the g-CDot@NaCl composite phosphors were applied as color conversion layers for WLEDs

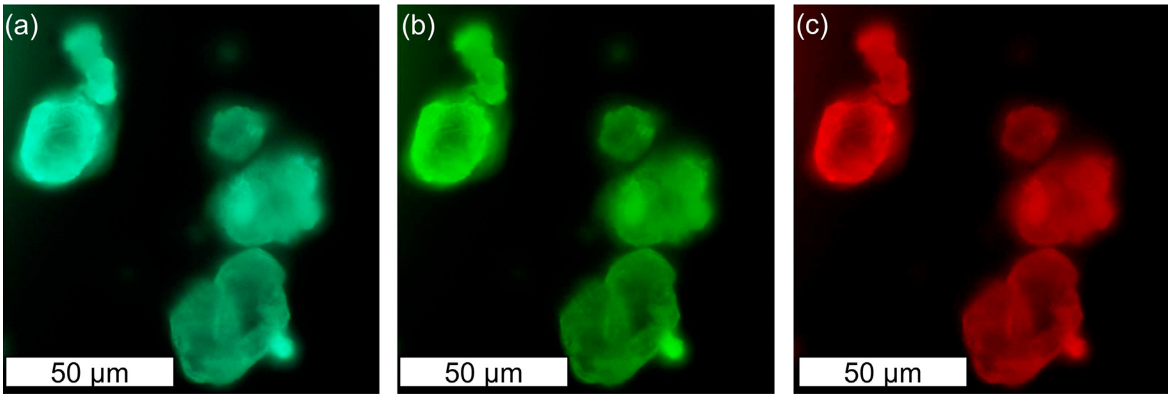

Fig. 3. Fluorescent images of g-CDot@NaCl composite phosphors through fluorescence microscope under (a) UV, (b) blue and (c) green exciting, respectively. The exposure time is 100, 150 and 6000 ms, respectively. (For interpretation of the references to colour in this figure legend, the reader is referred to the web version of this article.)

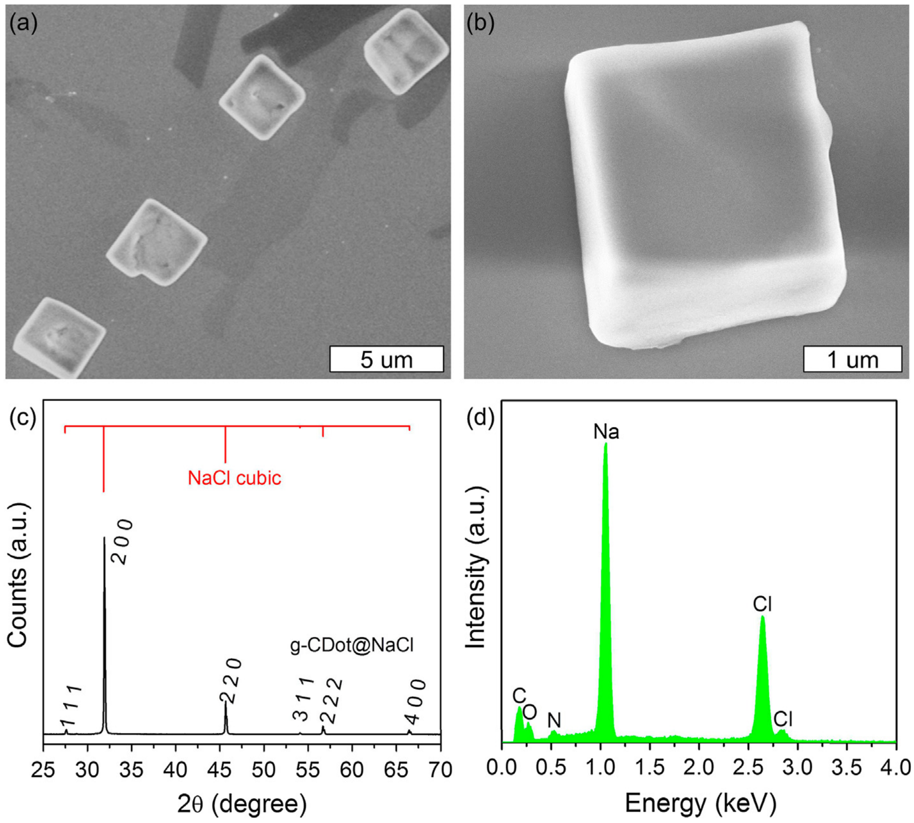

Fig. 4. (a and b) SEM images of g-CDot@NaCl composite phosphors. (c) XRD patterns of bare NaCl (red line) and g-CDot@NaCl composite phosphors (black line). (d) EDS pattern of g-CDot@NaCl composite phosphors. (For interpretation of the references to colour in this figure legend, the reader is referred to the web version of this article.)

(Fig. 6). The mixtures, which are prepared with the mass ratios of g-CDot@NaCl composite phosphors and PDMS ranging from 4:1 to 2:1, cover the InGaN LED chips. Meaningfully, through adjusting the amount of the composite phosphors, PL reabsorption among g-CDots could be controlled, and therewith the WLEDs with different CIE coordinates are obtained [51]. In LEDs, the InGaN chip could emit blue light, which can excite the adjacent composite phosphors. Then, along the path of light transmission, the high energy emission could be progressively absorbed (*i.e.*, PL emission reabsorption). As a result, the higher the mass ratio of the composite phosphors leads to more obvious reabsorption [41,52]. This is also validated by the emission spectra of LEDs, where the emission peaks red-shift upon increasing the contents of composite phosphors (Fig. 6a–c). As seen from Fig. 6b, CIE coordination and

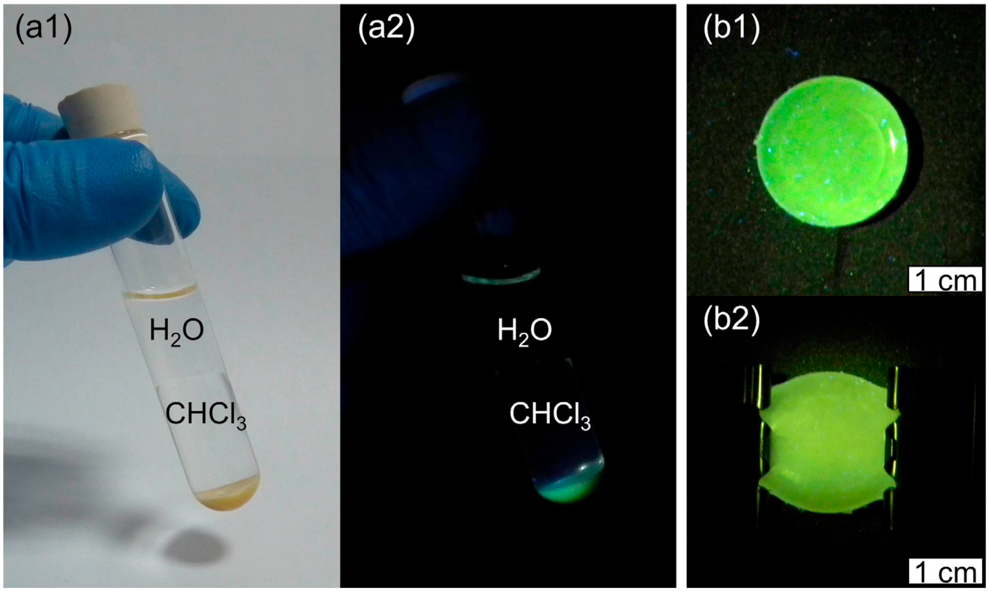

Fig. 5. (a) Images of g-CDot@NaCl composite phosphors in chloroform, under day light (a1) and UV light (a2). (b) Fluorescent images of g-CDot@NaCl composite phosphors in PDMS. (b1) Relaxed state, and (b2) tensional state.

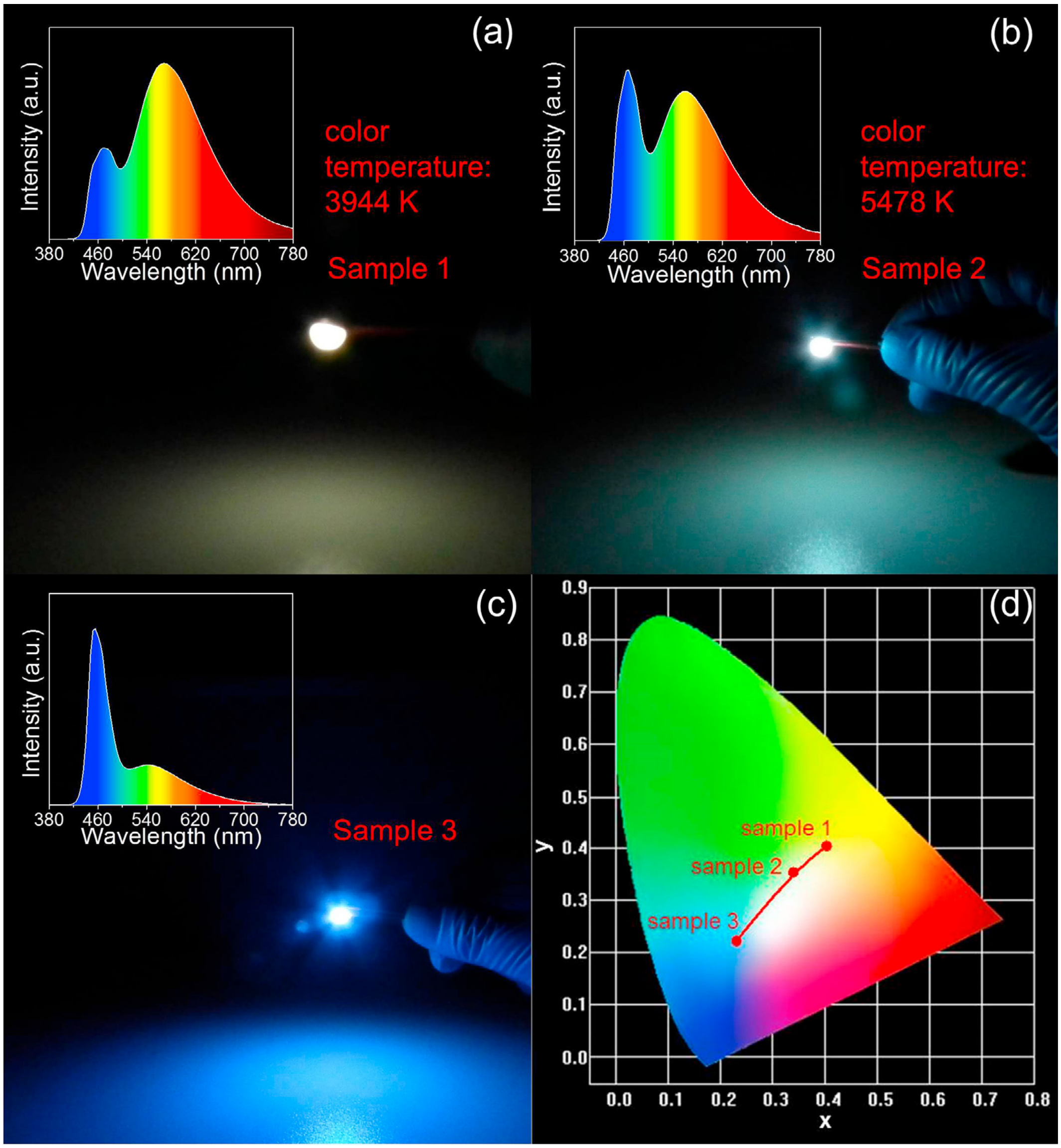

Fig. 6. Photographs of the working WLEDs based on the g-CDot@NaCl composite phosphors with different color temperatures, where the mass ratios of phosphors to PDMS are (a) 4:1, (b) 3:1 and (c) 2:1, respectively. Illustrations in (a–c) are corresponding emission spectra of WLEDs. (d) CIE chromaticity diagram showing (x, y) color coordinates of the three WLEDs. The color temperature of simple 3 is too high to be calculated. (For interpretation of the references to colour in this figure legend, the reader is referred to the web version of this article.)

color temperature of WLED are (0.33, 0.37) and 5478 K. Furthermore, a warm WLED prototype is achieved, whose CIE coordinates and color temperature is (0.40, 0.43) and 3944 K (Fig. 6a), respectively.

3. Conclusions

In conclusion, g-CDot@NaCl composite phosphors were prepared *via* embedding g-CDots in NaCl crystals. Our study shows that g-CDots embedded in NaCl matrices exhibit excellent photostability, resistance to organic solvents, as well as structural stability. After continuous UV irradiations for 65 min, the PL intensity of phosphors still preserves 85%. All of these allow the g-CDot@NaCl composite phosphors to be used for WLEDs with tunable color temperatures. We prospect that this synthetic methodology also expands the way of CDots for wider applications in many other fields.

4. Materials and methods

4.1. Materials

NaCl (99.5%), urea (99%), and citric acid (99.5%) were purchased from Dingshengxin, Macklin and Aladdin, respectively. The material of encapsulation we used was polydimethylsiloxane (PDMS) elastomer kits (Sylgard 184), which were obtained from Dow Corning (Midland, MI). All of them were not purified before being used.

4.2. Synthesis of CDots with green emission

3 g-CDots were prepared according to our precious work [33]. 3 g citric acid and 6 g urea were added into 20 ml deionized water to form transparent solution. Then the mixture was deeply heated about 5 min in a domestic 650 W microwave oven, during which the mixture varied in color and state that from a colorless liquid

to a brown and finally dark-brown solid, indicating the formation of g-CDots. After that, g-CDots were re-dissolved in deionized water, and purified in a centrifuge to remove the aggregated particles at the speed of 8000 rpm for 5 min. Finally, the yellow-brown solution was obtained.

4.3. Preparation of g-CDot@NaCl composite phosphors

100 ml of 0.5 mg/ml g-CDots aqueous solution was heated to 90 °C and mixed with 38.2 g NaCl in the 500 ml beaker to form saturated solution. Then the solution was cooled down to room temperature naturally. After 2 days later, g-CDot@NaCl composite microcrystals were obtained. The microcrystals on the beaker were removed gently, then washed with ethanol, dried and ground into powders for further being used.

4.4. Preparation of disc with g-CDot@NaCl composite phosphors and PDMS

g-CDot@NaCl composite phosphors were added into PDMS at a mass ratio of 3:1, stirring uniformly. Then the mixture was put into a cap of 50 ml centrifuge tube. The air in the mixture was removed by vacuum oven. The mixture was further baked at 80 °C for 1 h. Finally, a disc, which was composed of phosphors and PDMS, was obtained. The disc was stretched to test the stability of g-CDot@NaCl composite phosphors in the tensional state.

4.5. Fabrication of WLEDs from g-CDot@NaCl composite phosphors

InGaN chips with 450 nm light were used as the WLEDs base. Mixtures, which were composed of g-CDot@NaCl composite phosphors and PDMS with mass ratios of 4:1, 3:1 and 2:1, respectively, were used as color conversion layers. The InGaN chips were covered with the foremost prepared mixtures, and cured at 80 °C for 1 h. After that, the WLEDs based on g-CDot@NaCl composite phosphors were obtained.

4.6. Characterization

JEOL FESEM 6700F electron microscope with primary electron energy of 3 kV. Siemens D5005 diffractometer was used to record the X-ray powder diffraction (XRD) of g-CDot@NaCl composite phosphors. C2+ confocal microscope system (Nikon confocal instruments) was used as the instrument to take the fluorescence microscopy images. Inca X-Max instrument (Oxford Instruments) was used to get the energy dispersive spectra (EDS) and elemental mapping of g-CDot@NaCl composite phosphors. The calibrated integrating sphere in FLS920 spectrometer was used for carrying out the PLQYs of g-CDot@NaCl composite phosphors.

Author contributions

The manuscript was written through contributions of all authors. All authors have given approval to the final version of the manuscript.

Acknowledgment

This work is supported by the National Natural Science Foundation of China Nos. 51602304, and 51572128. Outstanding young scientists program of Chinese Academy of Sciences, Youth Innovation Promotion Association of CAS, Jilin Province Science and Technology Research Project No. 20160520008JH, 20170101042JC, 20170101191JC, and 20150519003JH.

Appendix A. Supplementary material

Supplementary data associated with this article can be found, in the online version, at http://dx.doi.org/10.1016/j.jcis.2017.03.007.

References

[1] S. Landau, J. Erion, Automotive: car makers embrace LED signals, Nat. Photonics 1 (2007) 31–32.

[2] D.I. Son, B.W. Kwon, D.H. Park, W.S. Seo, Y. Yi, B. Angadi, C.L. Lee, W.K. Choi, Emissive zno-graphene quantum dots for white-light-emitting diodes, Nat. Nanotechnol. 7 (2012) 465–471.

[3] H. Choi, S.-J. Ko, Y. Choi, P. Joo, T. Kim, B.R. Lee, J.-W. Jung, H.J. Choi, M. Cha, J.-R. Jeong, I.-W. Hwang, M.H. Song, B.-S. Kim, J.Y. Kim, Versatile surface plasmon resonance of carbon-dot-supported silver nanoparticles in polymer optoelectronic devices, Nat. Photonics 7 (2013) 732–738.

[4] J.Y. Tsao, Solid-state lighting: lamps, chips, and materials for tomorrow, IEEE Circ. Dev. 20 (2004) 28–37.

[5] Q.Q. Dai, C.E. Duty, M.Z. Hu, Semiconductor-nanocrystals-based white light-emitting diodes, Small 6 (2010) 1577–1588.

[6] A.L. Rogach, N. Gaponik, J.M. Lupton, C. Bertoni, D.E. Gallardo, S. Dunn, N.L. Pira, M. Paderi, P. Repetto, S.G. Romanov, C. O'Dwyer, C.M.S. Torres, A. Eychmüller, Light-emitting diodes with semiconductor nanocrystals, Angew. Chem. Int. Ed. 47 (2008) 6538–6549.

[7] E. Jang, S. Jun, H. Jang, J. Lim, B. Kim, Y. Kim, White-light-emitting diodes with quantum dot color converters for display backlights, Adv. Mater. 22 (2010) 3076–3080.

[8] X.Y. Xu, R. Ray, Y.L. Gu, H.J. Ploehn, L. Gearheart, K. Raker, W.A. Scrivens, Electrophoretic analysis and purification of fluorescent single-walled carbon nanotube fragments, J. Am. Chem. Soc. 126 (2004) 12736–12737.

[9] Y.P. Sun, B. Zhou, Y. Lin, W. Wang, K.A.S. Fernando, P. Pathak, M.J. Meziani, B.A. Harruff, X. Wang, H.F. Wang, P.G. Luo, H. Yang, M.E. Kose, B.L. Chen, L.M. Veca, S.Y. Xie, Quantum-sized carbon dots for bright and colorful photoluminescence, J. Am. Chem. Soc. 128 (2006) 7756–7757.

[10] L. Cao, X. Wang, M.J. Meziani, F.S. Lu, H.F. Wang, P.G. Luo, Y. Lin, B.A. Harruff, L. M. Veca, D. Murray, S.Y. Xie, Y.P. Sun, Carbon dots for multiphoton bioimaging, J. Am. Chem. Soc. 129 (2007) 11318–11319.

[11] R.L. Liu, D.Q. Wu, S.H. Liu, K. Koynov, W. Knoll, Q. Li, An aqueous route to multicolor photoluminescent carbon dots using silica spheres as carriers, Angew. Chem. Int. Ed. 48 (2009) 4598–4601.

[12] H. Peng, J. Travas-Sejdic, Simple aqueous solution route to luminescent carbogenic dots from carbohydrates, Chem. Mater. 21 (2009) 5563–5565.

[13] S.T. Yang, L. Cao, P.G. Luo, F.S. Lu, X. Wang, H.F. Wang, M.J. Meziani, Y.F. Liu, G. Qi, Y.P. Sun, Carbon dots for optical imaging in vivo, J. Am. Chem. Soc. 131 (2009) 11308–11309.

[14] S.N. Baker, G.A. Baker, Luminescent carbon nanodots: emergent nanolights, Angew. Chem. Int. Ed. 49 (2010) 6726–6744.

[15] Y.X. Fang, S.J. Guo, D. Li, C.Z. Zhu, W. Ren, S.J. Dong, E.K. Wang, Easy synthesis and imaging applications of cross-linked green fluorescent hollow carbon nanoparticles, ACS Nano 6 (2011) 400–409.

[16] Y. Li, Y. Hu, Y. Zhao, G.Q. Shi, L. Deng, Y.B. Hou, L.T. Qu, An electrochemical avenue to green-luminescent graphene quantum dots as potential electron-acceptors for photovoltaics, Adv. Mater. 23 (2011) 776–780.

[17] H.Q. Tao, K. Yang, Z. Ma, J.M. Wan, Y.J. Zhang, Z.H. Kang, Z. Liu, In vivo nir fluorescence imaging, biodistribution, and toxicology of photoluminescent carbon dots produced from carbon nanotubes and graphite, Small 8 (2011) 281–290.

[18] X.W. Xu, K. Zhang, L. Zhao, C. Li, W.H. Bu, Y.Q. Shen, Z.Y. Gu, B. Chang, C.Y. Zheng, C.T. Lin, H.C. Sun, B. Yang, Aspirin-based carbon dots, a good biocompatibility of material applied for bioimaging and anti-inflammation, ACS Appl. Mater. Interf. 8 (2016) 32706–32716.

[19] D. Li, D. Han, S.N. Qu, L. Liu, P.T. Jing, D. Zhou, W.Y. Ji, X.Y. Wang, T.F. Zhang, D.Z. Shen, Supra-(carbon nanodots) with a strong visible to near-infrared absorption band and efficient photothermal conversion, Light Sci. Appl. 5 (2016) e16120.

[20] D. Zhou, D. Li, P.T. Jing, Y.C. Zhai, D.Z. Shen, S.N. Qu, A.L. Rogach, Conquering aggregation-induced solid-state luminescence quenching of carbon dots through a carbon dots-triggered silica gelation process, Chem. Mater 29 (2017) 1779–1787.

[21] F. Wang, Y.H. Chen, C.Y. Liu, D.G. Ma, White light-emitting devices based on carbon dots' electroluminescence, Chem. Commun. 47 (2011) 3502–3504.

[22] F. Wang, Z. Xie, H. Zhang, C.Y. Liu, Y.G. Zhang, Highly luminescent organosilane-functionalized carbon dots, Adv. Funct. Mater. 21 (2011) 1027–1031.

[23] A.B. Bourlinos, R. Zbořil, J. Petr, A. Bakandritsos, M. Krysmann, E.P. Giannelis, Luminescent surface quaternized carbon dots, Chem. Mater. 24 (2012) 6–8.

[24] X. Guo, C.F. Wang, Z.Y. Yu, L. Chen, S. Chen, Facile access to versatile fluorescent carbon dots toward light-emitting diodes, Chem. Commun. 48 (2012) 2692–2694.

[25] B. Kong, A.W. Zhu, C.Q. Ding, X.M. Zhao, B. Li, Y. Tian, Carbon dot-based inorganic–organic nanosystem for two-photon imaging and biosensing of pH variation in living cells and tissues, Adv. Mater. 24 (2012) 5844–5848.

[26] M.J. Krysmann, A. Kelarakis, P. Dallas, E.P. Giannelis, Formation mechanism of carbogenic nanoparticles with dual photoluminescence emission, J. Am. Chem. Soc. 134 (2012) 747–750.
[27] Z. Xie, F. Wang, C.Y. Liu, Organic-inorganic hybrid functional carbon dot gel glasses, Adv. Mater. 24 (2012) 1716–1721.
[28] P. Yu, X.M. Wen, Y.R. Toh, J. Tang, Temperature-dependent fluorescence in carbon dots, J. Phys. Chem. C 116 (2012) 25552–25557.
[29] A.W. Zhu, Q. Qu, X.L. Shao, B. Kong, Y. Tian, Carbon-dot-based dual-emission nanohybrid produces a ratiometric fluorescent sensor for in vivo imaging of cellular copper ions, Angew. Chem. Int. Ed. 51 (2012) 7185–7189.
[30] P.C. Chen, Y.N. Chen, P.C. Hsu, C.C. Shih, H.T. Chang, Photoluminescent organosilane-functionalized carbon dots as temperature probes, Chem. Commun. 49 (2013) 1639–1641.
[31] W. Kwon, S. Do, J. Lee, S. Hwang, J.K. Kim, S.W. Rhee, Freestanding luminescent films of nitrogen-rich carbon nanodots toward large-scale phosphor-based white-light-emitting devices, Chem. Mater. 25 (2013) 1893–1899.
[32] X. Zhang, F. Wang, H. Huang, H.T. Li, X. Han, Y. Liu, Z.H. Kang, Carbon quantum dot sensitized TiO_2 nanotube arrays for photoelectrochemical hydrogen generation under visible light, Nanoscale 5 (2013) 2274–2278.
[33] X.Y. Zhang, Y. Zhang, Y. Wang, S. Kalytchuk, S.V. Kershaw, Y.H. Wang, P. Wang, T.Q. Zhang, Y. Zhao, H.Z. Zhang, T. Cui, Y.D. Wang, J. Zhao, W.W. Yu, A.L. Rogach, Color-switchable electroluminescence of carbon dot light-emitting diodes, ACS Nano 7 (2013) 11234–11241.
[34] L. Zhou, Z.H. Li, Z. Liu, J.S. Ren, X.G. Qu, Luminescent carbon dot-gated nanovehicles for ph-triggered intracellular controlled release and imaging, Langmuir 29 (2013) 6396–6403.
[35] S.J. Zhu, Q.N. Meng, L. Wang, J.H. Zhang, Y.B. Song, H. Jin, K. Zhang, H.C. Sun, H. Y. Wang, B. Yang, Highly photoluminescent carbon dots for multicolor patterning, sensors, and bioimaging, Angew. Chem. Int. Ed. 52 (2013) 3953–3957.
[36] J.C. Bian, C. Huang, L.Y. Wang, T. Hung, W.A. Daoud, R.Q. Zhang, Carbon dot loading and TiO_2 nanorod length dependence of photoelectrochemical properties in carbon dot/TiO_2 nanorod array nanocomposites, ACS Appl. Mater. Interf. 6 (2014) 4883–4890.
[37] C.Q. Ding, A.W. Zhu, Y. Tian, Functional surface engineering of c-dots for fluorescent biosensing and in vivo bioimaging, Acc. Chem. Res. 47 (2014) 20–30.
[38] K. Junka, J.Q. Guo, I. Filpponen, J. Laine, O.J. Rojas, Modification of cellulose nanofibrils with luminescent carbon dots, Biomacromolecules 15 (2014) 876–881.
[39] W. Kwon, G. Lee, S. Do, T. Joo, S.W. Rhee, Size-controlled soft-template synthesis of carbon nanodots toward versatile photoactive materials, Small 10 (2014) 506–513.
[40] S.H. Song, M.H. Jang, J. Chung, S.H. Jin, B.H. Kim, S.H. Hur, S. Yoo, Y.H. Cho, S. Jeon, Highly efficient light-emitting diode of graphene quantum dots fabricated from graphite intercalation compounds, Adv. Opt. Mater. 2 (2014) 1016–1023.
[41] Y. Wang, S. Kalytchuk, Y. Zhang, H.C. Shi, S.V. Kershaw, A.L. Rogach, Thickness-dependent full-color emission tunability in a flexible carbon dot ionogel, J Phys. Chem. Lett. 5 (2014) 1412–1420.
[42] Y.F. Wang, A.G. Hu, Carbon quantum dots: synthesis, properties and applications, J. Mater. Chem. C 2 (2014) 6921–6939.
[43] T.F. Yeh, C.Y. Teng, S.J. Chen, H. Teng, Nitrogen-doped graphene oxide quantum dots as photocatalysts for overall water-splitting under visible light illumination, Adv. Mater. 26 (2014) 3297–3303.
[44] Y.H. Chen, B.F. Lei, M.T. Zheng, H.R. Zhang, J.L. Zhuang, Y.L. Liu, A dual-emitting core-shell carbon dot-silica-phosphor composite for white light emission, Nanoscale 7 (2015) 20142–20148.
[45] X.M. Li, M.C. Rui, J.Z. Song, Z.H. Shen, H.B. Zeng, Carbon and graphene quantum dots for optoelectronic and energy devices: a review, Adv. Funct. Mater. 25 (2015) 4929–4947.
[46] Y. Wang, S. Kalytchuk, L.Y. Wang, O. Zhovtiuk, K. Cepe, R. Zboril, A.L. Rogach, Carbon dot hybrids with oligomeric silsesquioxane: solid-state luminophores with high photoluminescence quantum yield and applicability in white light emitting devices, Chem. Commun. 51 (2015) 2950–2953.
[47] M.Y. Sun, S.N. Qu, Z.D. Hao, W.Y. Ji, P.T. Jing, H. Zhang, L.G. Zhang, J.L. Zhao, D.Z. Shen, Towards efficient solid-state photoluminescence based on carbon-nanodots and starch composites, Nanoscale 6 (2014) 13076–13081.
[48] S.N. Qu, X.Y. Liu, X.Y. Guo, M.H. Chu, L.G. Zhang, D.Z. Shen, Amplified spontaneous green emission and lasing emission from carbon nanoparticles, Adv. Funct. Mater. 24 (2014) 2689–2695.
[49] D. Zhou, Y.C. Zhai, S.N. Qu, D. Li, P.T. Jing, W.Y. Ji, D.Z. Shen, A.L. Rogach, Electrostatic assembly guided synthesis of highly luminescent carbon-nanodots@BaSO4 hybrid phosphors with improved stability. Small. doi: http://dx.doi.org/10.1002/smll.201602055.
[50] A. Sciortino, E. Marino, B. Dam, P. Schall, M. Cannas, F. Messina, Solvatochromism unravels the emission mechanism of carbon nanodots, J Phys. Chem. Lett. 7 (2016) 3419–3423.
[51] D. Zhou, H.Y. Zou, M. Liu, K. Zhang, Y. Sheng, J.L. Cui, H. Zhang, B. Yang, Surface ligand dynamics-guided preparation of quantum dots-cellulose composites for light-emitting diodes, ACS Appl. Mater. Interf. 7 (2015) 15830–15839.
[52] C. Sun, Y. Zhang, S. Kalytchuk, Y. Wang, X.Y. Zhang, W.Z. Gao, J. Zhao, K. Cepe, R. Zboril, W.W. Yu, A.L. Rogach, Down-conversion monochromatic light-emitting diodes with the color determined by the active layer thickness and concentration of carbon dots, J. Mater. Chem. C 3 (2015) 6613–6615.